JOURNAL OF VIROLOGY, June 1993, p. 3095–3102
0022-538X/93/063095-08$02.00/0

Vol. 67, No. 6

# Synthesis and Assembly of Hepatitis A Virus-Specific Proteins in BS-C-1 Cells

STEVEN V. BOROVEC AND DAVID A. ANDERSON*

*Hepatitis Research Unit, Macfarlane Burnet Centre for Medical Research, Fairfield Hospital, Yarra Bend Road, Fairfield, Victoria 3078, Australia*

Received 17 December 1992/Accepted 23 February 1993

**To determine the mechanism for the delayed and inefficient replication of the picornavirus hepatitis A virus in cell culture, we studied the kinetics of synthesis and assembly of virus-specific proteins by metabolic labeling of infected BS-C-1 cells with L-[$^{35}$S]methionine and L-[$^{35}$S]cysteine. Sedimentation, electrophoresis, and autoradiography revealed the presence of virions, provirions, procapsids, and 14S (pentameric) subunits. Virions and provirions contained VP1, VP0, VP2, and VP3; procapsids contained VP1, VP0, and VP3; and pentamers contained PX, VP0, and VP3, as previously shown by immunoblotting (D. A. Anderson and B. C. Ross, J. Virol. 64:5284–5289, 1990). Under single-cycle growth conditions label was found in 14S subunits immediately after labeling from 15 to 18 h postinfection (p.i.); however, a proportion of labeled polyprotein was not cleaved and assembled into pentamers for a further 18 h. When analyzed at 72 h p.i., incorporation of label which flowed into virions was detected from 3 h p.i., with maximal uptake levels being observed from 12 to 15 h p.i. Viral antigen, infectious virus, and viral RNA were determined in parallel, with coincident peaks in these variables being observed 12 h after the period of maximum label uptake. It was also found that the lag between the synthesis of the viral polyprotein and assembly of viral particles was the same after labeling from either 12 to 15 or 27 to 30 h p.i. despite increased levels of viral RNA during this period, suggesting that factors additional to the level of RNA are involved in the restriction of viral replication. Sedimentation and immunoblot analysis revealed an additional protein of approximately 100 kDa containing both VP1- and VP2-reactive sequences and sedimenting slightly more slowly than 14S pentamers, which may represent intact P12A assembled into pentamers as has been reported for the P1 of some other picornaviruses (S. McGregor and R. R. Rueckert, J. Virol. 21:548–553, 1977). The results of this study suggest that cleavage of the hepatitis A virus polyprotein to produce pentamers is protracted (though not rate limiting) early in infection, while the assembly of pentamers into higher structures is a rapid process once sufficient viral RNA is produced for encapsidation.**

Hepatitis A virus (HAV) is an unusual picornavirus in that it is very stable under extremes of heat (28) and pH (27) and the replication cycle is slow and inefficient in cell culture. Most picornaviruses produce around 1,000 infectious particles per cell and rapidly produce cytopathic effects (25), whereas HAV produces only around 20 infectious particles, with most strains being noncytopathic (1). This unusual replicative inefficiency has hampered the development of an affordable vaccine, and many studies have addressed the mechanism(s) which acts to restrict the replication of the virus within the cell. Cho and Ehrenfeld (4) have suggested that asynchronous replication rather than slow replication per se is responsible for the protracted growth kinetics of HAV, while de Chastonay and Siegl (7) have observed a down-regulation of viral RNA synthesis following the initial period of replicative activity, perhaps related to the generation of defective interfering RNAs. Conversely, our initial observations of highly efficient encapsidation of HAV RNA (3) suggested that sequestration of RNA into virions limited the number of replicative intermediates and thus the growth rate and yield of the virus. We therefore suspected that the processing and assembly pathways of HAV proteins might differ from those of other picornaviruses.

The morphogenesis of picornaviruses begins with cleavage at the P1-P2 junction to yield a 5S protomer which may then assemble to form a pentameric subunit of 13S containing intact P1 (17, 18) or of 14S containing the products VP1, VP0, and VP3 (reviewed by Putnak and Phillips [20]). 14S subunits may self-assemble without RNA to form empty capsids (70S procapsids) or with positive-strand RNA to form provirions of approximately 150S. The maturation cleavage of all but one or two copies of VP0 to VP2 plus VP4 in the provirion yields a mature 160S virion (20). A previous study of HAV morphogenesis reported the presence of a unique structural protein precursor, PX (probably VP12A), assembled into pentamers (2), consistent with an unusual assembly pathway for this virus. However, while the processing of artificial HAV protein precursors in cell-free systems has been reported elsewhere (31), the kinetics of protein synthesis, processing, and assembly in HAV-infected cells has not previously been determined since infection of cells with HAV has a negligible effect on host cell macromolecular synthesis (7, 8, 16). This problem can be overcome by detecting virus particles after the purification of labeled infected cell lysates over sucrose gradients (2) together with suppression of host cell protein synthesis with hypertonic salt (26). In this report we describe the kinetics of synthesis, cleavage, and assembly of HAV-specific structural proteins during a single growth cycle and examine these processes as possible mechanisms involved in the restriction of replication.

## MATERIALS AND METHODS

**Cells and viruses.** HAV strain HM175A.2 and poliovirus type 1 (PV; Mahoney strain) were propagated in BS-C-1 cells and purified as described previously (2). Titration of infec-

* Corresponding author.

tious virus was by plaque assay or radioimmunofocus assay (RIFA) (15) as modified by Anderson (1).

**Single-cycle infection of cells.** Monolayers of BS-C-1 cells were inoculated with 10 infectious particles of HM175A.2 per cell for 1 h at 37°C, washed with normal saline, and maintained in Eagle's minimal essential medium at 37°C. The end of the adsorption period was considered to be 0 h. Cells were harvested by the addition of 0.5 ml of NPT (100 mM NaCl, 0.5% Nonidet P-40 [Sigma], 10 mM Tris [pH 7.4]) per 3-cm-diameter petri dish, after which nuclei were removed by centrifugation at 13,000 rpm in an MSE microcentrifuge. Cells infected with PV were maintained at 34°C, with other conditions being identical.

**Labeling of proteins with L-[$^{35}$S]methionine and L-[$^{35}$S]cysteine.** At various times cells were fed methionine- and cysteine-free Eagle's minimal essential medium (ICN Biomedicals Ltd., Costa Mesa, Calif.) for 3 h and then similar medium containing 150 μCi of L-[$^{35}$S]methionine per ml plus approximately 30 μCi of L-[$^{35}$S]cysteine per ml (Tran$^{35}$S label; ICN Biomedicals Ltd., Radiochemicals, Irvine Calif.; 1,150 Ci/mmol) for a further 3 h. Labeling medium was then removed, and cells were maintained in Eagle's minimal essential medium until harvest. Where indicated, host cell protein synthesis was suppressed by the addition of 200 mM excess NaCl (26) to the deficient media for the last 20 min of starvation and the duration of the labeling period. For the metabolic labeling of PV proteins, starvation and labeling periods were of 1-h duration. PV-infected cells were maintained at 34°C rather than 37°C in order to slow the replication cycle so that growth kinetics could be determined more precisely.

**Sucrose density gradient ultracentrifugation (SDGU).** Sodium dodecyl sulfate (SDS) was added to cell lysates to a final concentration of 1%. Samples (0.5 ml) were then layered on top of 5 to 30% (wt/vol) gradients of sucrose in NT (100 mM NaCl, 10 mM Tris [pH 7.4]). Gradients were centrifuged at 4°C in a Beckman SW41 rotor for 3 h at 35,000 rpm (150,000 × *g*) for the isolation of virions, provirions, and procapsids. For the isolation of 14S subunits, gradients of 5 to 20% sucrose in NT with centrifugation for 18 h at 37,000 rpm (170,000 × *g*) were used. Fractions (3 ml [for virions, provirions, and procapsids] or 0.5 ml [for 14S subunits]) were collected from the bottom of each tube.

**Electrophoresis.** Gradient fractions were mixed with 10 μl of bovine serum albumin (0.05% [wt/vol]; Commonwealth Serum Laboratories, Melbourne, Australia), and the protein was precipitated by adding 9 volumes of methanol at −20°C. Following an overnight incubation at −20°C, the precipitate was collected by centrifugation at 2,500 rpm in an MSE Mistral 4L centrifuge at −10°C and dried under vacuum. The pellet was dissolved in 30 μl of Laemmli buffer (2% SDS, 8% glycerol, 0.01% bromophenol blue, 5% 2-mercaptoethanol, 50 mM Tris [pH 6.8]) and then boiled for 5 min. Electrophoresis was performed with the Mini-Protean II apparatus (Bio-Rad, Richmond, Calif.). The SDS-polyacrylamide gel electrophoresis (SDS-PAGE) buffer system of Laemmli (13) was used with 12% acrylamide and an acrylamide-bisacrylamide ratio of 30:0.8. For the electrophoresis of HAV proteins urea was added to the gels to a final concentration of 3.5 M (23). Samples (10 μl) in Laemmli buffer were electrophoresed at 150 V until the dye front reached the bottom of the gel.

**Immunoblot analysis and fluorography.** Proteins were transferred to nitrocellulose membranes (Hybond C-extra; Amersham) for 30 min at 15 V in a Trans-Blot semidry transfer apparatus (Bio-Rad) with a buffer of 20% methanol, 0.15 M glycine, and 25 mM Tris (pH 7.5). Filters were dried at room temperature and then incubated for 1 h with shaking in 0.1 M Tris (pH 7.5) containing 3% (wt/vol) casein. After a brief wash in TBST (0.1 M NaCl, 0.1 M Tris [pH 7.5], 0.05% Tween 20), HAV-specific proteins were detected with a 1-h incubation at 37°C with rabbit antisera raised to recombinant HAV proteins containing sequences of VP1 and VP2 (22, 23) diluted 1:10,000 and 1:20,000, respectively, in TBST with 1% casein. Unbound antibody was removed by two brief washes in TBST followed by a 15-min wash with gentle agitation. Horseradish peroxidase-labeled goat anti-rabbit immunoglobins (Amersham) were diluted 1:20,000 in TBST with 1% casein and incubated with the membrane for 1 h. Unbound antibody was again removed, and the presence of horseradish peroxidase was detected by enhanced chemiluminescence as per the manufacturer's instructions (Amersham). Membranes were then thoroughly washed in TBST to remove luminescence reagents before fluorography.

For fluorography, membranes were dried at 80°C for 10 min and briefly immersed in 20% (wt/vol) PPO (2,5-diphenyloxazole) in diethyl ether, dried at 20°C, and exposed to preflashed X-Omat RP film (Eastman Kodak Co., Rochester, N.Y.).

**Trichloroacetic acid (TCA) precipitation of radiolabeled proteins.** Ten microliters of sample in Laemmli buffer was applied to a 25-mm-diameter glass fiber disk (Gelman Sciences, Ann Arbor, Mich.) and allowed to dry overnight. Disks were then immersed in a solution of 10% (wt/vol) TCA at 4°C and kept on ice for 1 h. The disks were washed twice in 5% TCA and twice in 100% ethanol before drying at room temperature. Acid-precipitable $^{35}$S was then quantitated by scintillation counting using Optiphase HiSafe II scintillation fluid (LKB, Uppsala, Sweden).

**In situ radioimmunoassay.** The accumulation of HAV antigen was determined by infecting monolayers established on 25-mm-diameter coverslips. Duplicate coverslips were removed at intervals and fixed in acetone at 4°C for 2 min. Coverslips were dried at room temperature and stained with iodinated monoclonal antibody K3-4C8 as for the modified RIFA (1), and bound radioactivity was quantitated in a gamma counter.

**Indirect immunofluorescence.** HAV antigen in cells was detected by using monoclonal antibody K3-4C8 to stain acetone-fixed cells as previously described by Anderson et al. (3). PV antigen was detected in a similar manner with polyclonal antibodies raised in rabbits immunized with 200 μg of pure PV.

**Detection of HAV RNA.** HAV-specific positive-strand RNA was detected by using a $^{32}$P-labeled negative-strand RNA probe (2). Monolayers established in 33-cm-diameter petri dishes were harvested in 0.5 ml of NPT at various times postinfection (p.i.). After removal of nuclei, RNA was extracted from the cytoplasmic lysates by a modification of the phenol-chloroform method of Coulepis et al. (6). Samples were adjusted to contain 2% (wt/vol) SDS and NET (100 mM NaCl, 10 mM EDTA, 10 mM Tris [pH 7.4]). To 200 μl of this lysate were added 20 μl of 2-mercaptoethanol, 200 μl of phenol-chloroform extraction buffer (0.5% SDS, 140 mM LiCl, 6 mM sodium acetate [pH 4.9]), and 200 μl of phenol-chloroform (50% [vol/vol] chloroform, 48% [vol/vol] water-saturated phenol, and 2% [vol/vol] 2-isobutanol). After shaking for 5 min at 24°C the mixture was centrifuged at 15,000 × *g* for 15 min at 4°C. The aqueous phase was mixed with 10 μl of glycogen (2.5 mg/ml), 2.5 volumes of 95% ethanol containing 57 mM sodium acetate were added, and the samples were held at −20°C overnight. The precipitate was collected

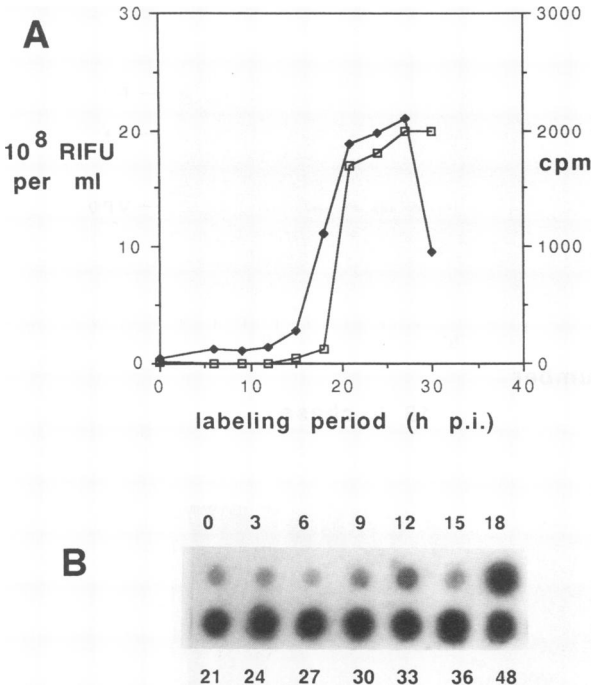


FIG. 1. (A) Single-cycle growth kinetics of HAV strain HM175A.2 in BS-C-1 cells. Infectious virus was measured by RIFA (□) and HAV antigen in situ radioimmunoassay (◆). For the RIFA, cells were harvested in NPT at various times p.i. and titers of infectious virus in the lysate were determined as described in Materials and Methods. For the in situ radioimmunoassay, monolayers were fixed in acetone before staining with $^{125}$I-labeled monoclonal antibody K3-4C8 and subsequent counting. RIFU, radioimmunofocus forming units. (B) Accumulation of HAV-specific positive-strand RNA during a single cycle of growth. RNA was extracted from replicate infected monolayers as described in Materials and Methods. After immobilization on nitrocellulose membranes, viral RNA was detected with HAV-specific $^{32}$P-labeled negative-strand RNA probes. Hours p.i. are indicated above and below.

by centrifugation at 15,000 × *g* for 60 min at 4°C, dried at 24°C under vacuum, and redissolved in 100 μl of RNase-free water. Samples were mixed with 3 volumes of FSSC (6.1 M formaldehyde, 3 M NaCl, 0.3 M sodium citrate, pH 7.0), heated at 60°C for 15 min, and immobilized on Hybond C-extra (Amersham) with a Bio-Dot apparatus (Bio-Rad).

## RESULTS

**Single-cycle growth kinetics.** In order to relate the kinetics of radiolabel uptake to other replicative events, parallel infected monolayers were analyzed for viral antigen, RNA, and infectious virus for the duration of pulse-chase experiments. As previously found for the fast-growing HM175A.2 strain of HAV (3), infectious virus and antigen began to increase at 12 h p.i., with both peaking at 27 h (Fig. 1A). Viral RNA was also found to increase logarithmically from 12 h (part of the sample was lost at 15 h), but a clear peak in this parameter was not seen on this occasion (Fig. 1B). Previous experiments have, however, repeatedly shown RNA to peak at 27 h p.i., concurrently with antigen and infectious virus (3). The sharp drop in viral antigen noted between 27 and 30 h p.i. was the result of cell detachment from the coverslip due to cytopathic effect.

Detection of antigen by immunofluorescence revealed similar kinetics, with antigen being first detected at 12 h p.i. with a peak at 27 h (results not shown).

**Metabolic labeling of 14S subunits.** In order to determine the kinetics of HAV protein synthesis and processing in infected cells, it is necessary to detect the primary products of such processing (monomers or pentamers) as well as final products (virions and procapsids), the accumulation of which involves other factors, such as the availability of RNA. As HAV has no effect on host cell protein synthesis and the primary products are expected to have sedimentation coefficients similar to those of many cellular proteins, host cell protein synthesis was minimized by exposing monolayers to 200 mM excess NaCl for the final 20 min of starvation as well as for the period of labeling. The presence of excess salt throughout a 72-h growth cycle was previously shown to have no effect on the yield of HAV products (3a).

Replicate infected monolayers established in 14-cm-diameter petri dishes were radiolabeled from 15 to 18 h p.i. One culture was chased for 0 h, and the other was chased for 18 h. Cell lysates were harvested and sedimented over sucrose as described in Materials and Methods, with the resultant fractions being analyzed by immunoblotting (Fig. 2A). Following the immunological detection of viral proteins by enhanced chemiluminescence, the membrane was fluorographed to detect metabolically labeled proteins (Fig. 2B). Comparison of these two figures allows radiolabeled proteins to be identified as viral or cellular. Fractions 5 to 8 contain the 14S subunits which can be identified by the presence of the precursor PX (40 kDa) in place of its product, VP1 (33 kDa) (2), which is produced in significant amounts only after assembly into procapsids and provirions. The detection of pentamers after a 3-h labeling with no subsequent chase period demonstrates that some cleavage of the viral polyprotein occurs within 3 h. After chasing for 18 h, similar amounts of radiolabeled pentamers which may represent either inefficient conversion into virions or procapsids or continued processing of polyprotein synthesized during the labeling period balanced with accretion of pentamers into larger forms were detected. Monomeric intermediates (5S) were not detected by labeling or immunoblotting; however, immunoblotting revealed a protein of approximately 100 kDa which sediments as a broad peak, slightly more slowly than pentamers containing PX, VP0, and VP3. This protein reacted with antisera to both VP1 and VP2 in separate immunoblots (results not shown), and its size is consistent with the P12A region of the HAV polyprotein (PX plus VP0 plus VP3 [2]). The sedimentation coefficient of this protein suggests that it exists as a multimer and may be analogous to the 13S pentamers of P1 described for other picornaviruses (17, 18).

**Metabolic labeling of HAV and PV virions and procapsids.** As shown previously (3) (Fig. 1), the accumulation of HAV-specific antigens and RNA coincides with the production of infectious virus, and we have examined whether the synthesis of proteins which are subsequently assembled into virions and procapsids follows a similar temporal pattern. Monolayers established in 3-cm-diameter petri dishes were infected, later starved, and then exposed to L-[$^{35}$S]methionine (150 μCi/ml) for consecutive 3-h periods. All monolayers were harvested at 72 h p.i., with viral particles being purified by SDGU.

Fractions from the gradients were subjected to SDS-PAGE followed by fluorography (Fig. 3). The first 3-ml fraction from the bottom of the gradient (Fig. 3B) contains predominantly virions (2) (VP1, VP2 > VP0, and VP3) and

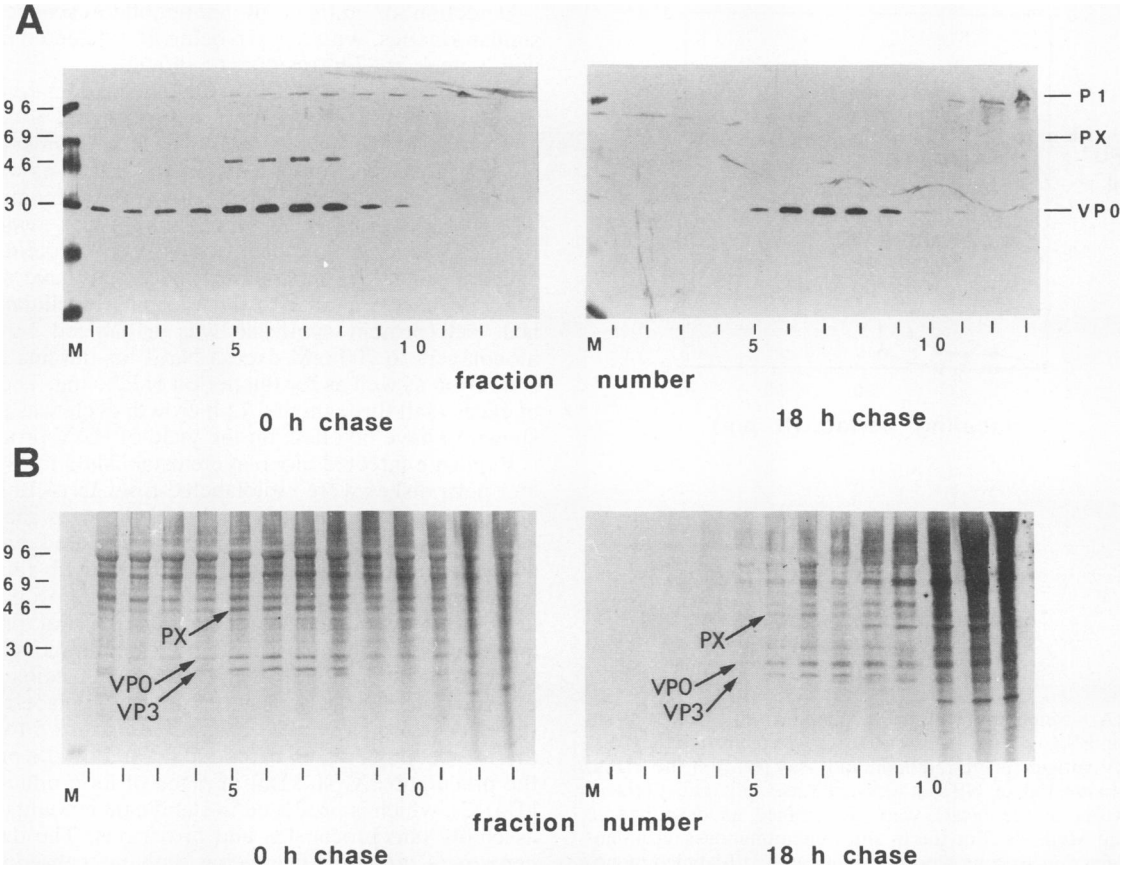


FIG. 2. Accumulation of pentameric subunits of HAV in BS-C-1 cells. Infected cells were labeled with [$^{35}$S]methionine from 15 to 18 h p.i. and chased for either 0 or 18 h. Cell lysates were centrifuged at 170,000 × *g* for 18 h at 4°C on linear 5 to 20% sucrose gradients in Beckman SW41 tubes. Fractions (0.5 ml) were collected from the bottom of each gradient, with proteins being methanol precipitated prior to their separation by SDS-PAGE and transfer to nitrocellulose. (A) HAV-infected cells harvested at 18 (left) and 36 (right) h p.i. Virus-specific proteins were detected by immunoblotting using antibodies raised against VP1 and VP2. (B) Fluorograph of the same membrane after immunoblotting. Lanes M, molecular mass markers (sizes are indicated at the left in kilodaltons). The identities of viral proteins detected are indicated.

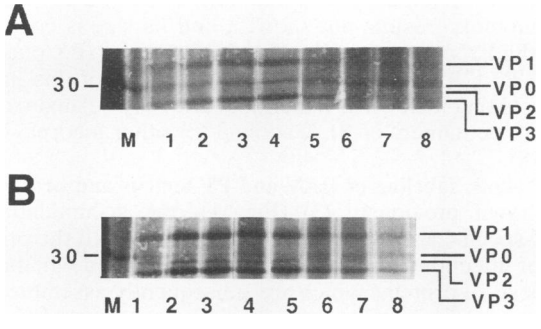


FIG. 3. Kinetics of incorporation of [$^{35}$S]methionine into viral particles. Infected cells were labeled for 3-h periods and harvested at 72 h p.i. Lysates were sedimented over 5 to 30% sucrose gradients at 150,000 × *g* for 3 h at 4°C. Fractions (3 ml) were taken from the bottom of each tube, with proteins being precipitated, electrophoresed, and electroblotted as described in Materials and Methods. (A) Procapsid-containing fraction; (B) virion- and provirion-containing fraction. Lanes 1 to 8, consecutive 3-h labeling periods beginning at 3 to 6 h p.i.; lanes M, molecular weight markers (size indicated to the left in kilodaltons).

provirions (VP1, VP0 > VP2, and VP3), with the second 3 ml containing mainly procapsids (VP1, VP0, and VP3; Fig. 3A). Quantitation of label uptake was accomplished by densitometry of the fluorographs (Fig. 4A) and scintillation counting of TCA-precipitable material (Fig. 4B). The most efficient incorporation of radiolabel into proteins which subsequently assembled into virions was found to occur in the 12- to 15-h labeling period, while for empty capsids incorporation peaked earlier, at 6 to 9 h p.i. It should be noted that the parallel growth curve (Fig. 1) shows peaks in infectious virus, RNA, and antigen occurring at least 12 h after the period of maximum label uptake into virions. This experiment has been repeated three times, and while the absolute times for the peaks in label uptake into procapsids and virions can vary by 3 h, the peak for procapsids always precedes that for virions by 6 h. In addition, the maxima in viral growth parameters (antigen, RNA, and infectious virus) have consistently been found to occur at least 12 h after the peak label uptake period for virions.

Metabolic labeling of PV was accomplished in a manner identical to that used for HAV except that starvation and labeling periods were 1 h each and monolayers were harvested at 12 h p.i. In addition, the temperature of incubation was reduced to 34°C to allow for better resolution of the peak

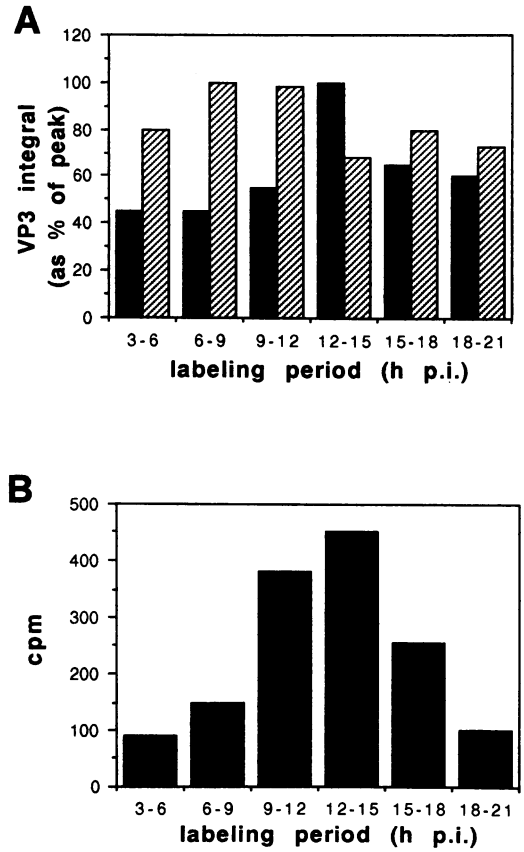


FIG. 4. Quantitation of radiolabel uptake into virions and procapsids. (A) Densitometry of VP3 bands seen in autoradiographs Fig. 3A (procapsids) (▨) and Fig. 3B (virions) (■); (B) scintillation counting of TCA-precipitable material present in aliquots of the virion-containing fractions from Fig. 3B.

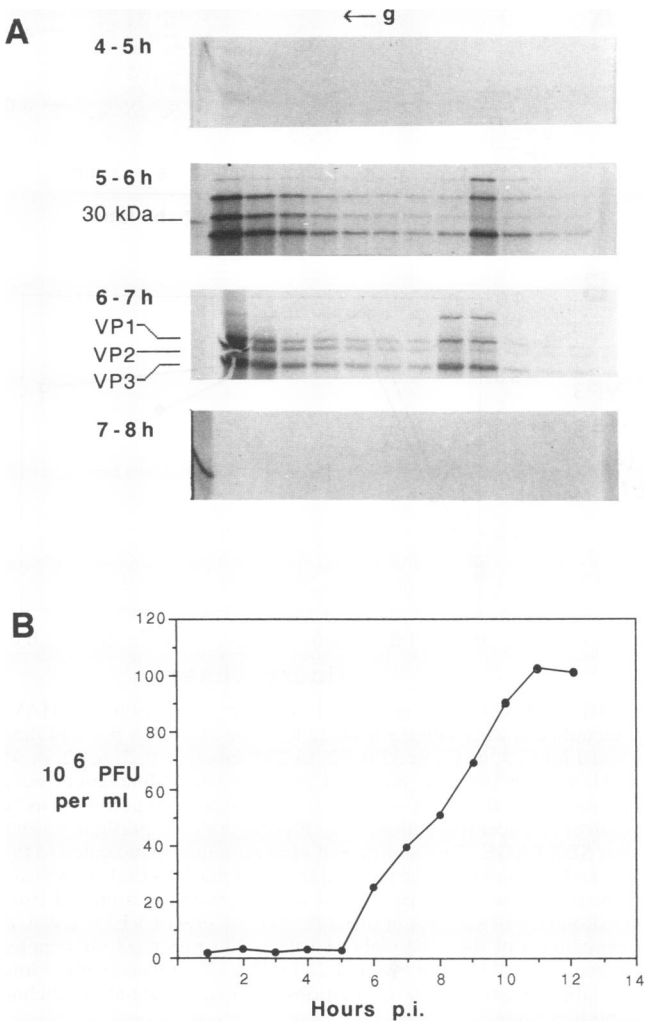


FIG. 5. (A) Kinetics of radiolabel uptake for PV in BS-C-1 cells. Replicate cultures of PV-infected cells were exposed to [$^{35}$S]methionine for consecutive 1-h periods and chased until 12 h p.i. Cell lysates were sedimented over 5 to 30% sucrose gradients for 3 h at 170,000 × *g*, with 0.5-ml samples being taken from the bottom of the tube. Proteins were separated by SDS-PAGE and then transferred to nitrocellulose for fluorography. Molecular weight markers appear in the leftmost lanes. (B) PV plaque assay of cell lysates from parallel cultures.

uptake period (see Materials and Methods). Fluorography revealed that the peak period of radiolabel uptake occurred in the 5- to 7-h period (Fig. 5A), coinciding with a logarithmic increase in virus beginning at 5 h p.i. and reaching a maximum by 11 h (Fig. 5B). Immunofluorescence demonstrated the first appearance of PV antigen at 5 h p.i. (results not shown). Despite the lower incubation temperature and consequently protracted growth cycle of 11 h for PV, it can be seen that the flow of radiolabel into HAV virions is slow compared with that in PV-infected cells.

**Kinetics of virus assembly.** Monolayers established in 6-cm-diameter petri dishes were infected with HAV and labeled in a manner similar to that described above, with replicate cultures being pulse-labeled from 12 to 15 h or from 24 to 27 h p.i. Cells labeled during each period were chased then harvested after 0, 3, 6, 12, and either 41 (24- to 27-h group; 68 h total) or 57 (12- to 15-h group; 72 h total) h. Cell lysates were analyzed by SDGU and SDS-PAGE for labeled virions (Fig. 6A), which again shows more efficient labeling from 12 to 15 h p.i. The quantity of labeled virions was estimated from densitometry of VP1 or VP3 in each sample. The quantity at each time was then calculated as a percentage of the yield at 68 or 72 h p.i., with calculations based on VP1 (not shown) and VP3 (Fig. 6B) giving similar results. These results demonstrate that radiolabel chased through to virions at a similar rate from both the period of peak uptake (when RNA levels were low; Fig. 1) and later when RNA levels were higher but radiolabel uptake was less efficient.

## DISCUSSION

The slow and inefficient replication of HAV in cell culture contrasts strongly with most other picornaviruses and hampers large-scale, cost-effective production of viral antigen for diagnostic and vaccine uses. Numerous studies have examined the step(s) contributing to the restricted replication of HAV, with many hypotheses being proposed from the limited amount of information available (reviewed by Lemon [14]). While studies to date have focused mainly on the more easily detected viral antigens, RNA, and infectivity, the synthesis and processing of HAV proteins (as distinct from antigens) have been poorly studied until now. This has been

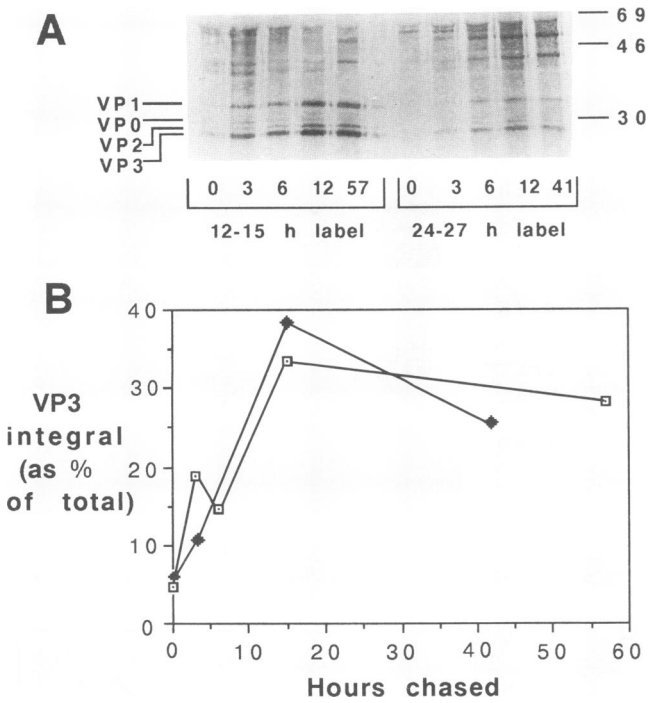


FIG. 6. Kinetics of radiolabel transfer into virions of HAV. Infected cells were labeled from 12 to 15 or 24 to 27 h p.i. and then chased for 0, 3, 6, 12, or 57 h (12- to 15-h label) or 0, 3, 6, 12, or 41 h (24- to 27-h label) as indicated for each lane. Monolayers were harvested in NPT, and virions were purified by sucrose density gradient ultracentrifugation. (A) Fluorograph of purified virions after SDS-PAGE. The identities of viral proteins are indicated to the left, and the masses of the molecular weight markers (not shown) are indicated to the right. (B) Rate of accumulation as estimated from densitometry of samples in panel A. The integral of VP3 is given as a percentage of the total yield of VP3 at 72 or 68 h p.i. in samples labeled from 12 to 15 h (◆) and 24 to 27 h (⊡), respectively. Note that label appears to flow into virions at an equal rate after labeling at both periods.

due to difficulties in detecting small amounts of viral product against the high background of cellular product seen after metabolic labeling: a result of the inability of HAV to inhibit host cell protein synthesis.

While in vitro studies have allowed the confirmation of 3C protease activity and some cleavage sites in the polyprotein (9, 11) as predicted by Cohen et al. (5), it is unclear whether these cleavages accurately reflect processing in the infected cell. To this end, in vivo work by Anderson and Ross (2) has shown that primary processing of the P1-P2 region of HAV was found to resemble that of cardioviruses and aphthoviruses (10, 30) rather than enteroviruses and rhinoviruses; however, these studies were unable to address the kinetics of protein processing and assembly.

In this report, the purification method of SDGU (2) in conjunction with hypertonic salt inhibition of cellular protein synthesis was used, and we have now detected metabolically radiolabeled structural proteins in the following forms: (i) 14S pentamers containing PX, VP0, and VP3 (Fig. 2B); (ii) procapsids containing VP1, VP0, and VP3 (Fig. 3A); and (iii) virions and provirions containing VP1, VP0, VP2, and VP3 (Fig. 3B). Labeling and detection of these species have allowed us to monitor for the first time the kinetics of capsid protein processing and assembly. Furthermore, immunoblot analysis has revealed an additional species of 100 kDa sedimenting at approximately 13S (Fig. 2A). This protein has an apparent molecular mass close to the 97 kDa which would be predicted for the P1 region plus the 2A portion of PX (2), is not found in uninfected cells, and reacts with both VP1- and VP2-specific antibodies in separate immunoblots (results not shown). We therefore believe this molecule to be the P12A region of the polyprotein, and its sedimentation is consistent with a multimeric structure such as a pentamer.

Immunoreactive material consistent with a 5S promoter was not detected in these or previous experiments (2). This may be due to its rapid assembly into pentamers from the cleavage products of the P12A region (PX, VP0, and VP3), so that at any time the concentration of this species is undetectably low in this system. However, our results suggest the further possibility that the protomer does not exist as a complex of VP0, VP3, and PX but rather exists as the intact P12A polyprotein. Five copies of this molecule may rapidly assemble to give a 13S particle (Fig. 2A, fractions 5 to 8), as detected in encephalomyocarditis virus- and rhinovirus-infected cells (17, 18). Internal cleavage of this 13S subunit by 3C protease may then occur to give the PX, VP0, and VP3 seen in the pentamer and an increase in sedimentation coefficient to 14S.

Whatever the immediate precursor of the 14S pentamer may be, the observation of labeled pentamers at the conclusion of the 15- to 18-h labeling period (Fig. 2B) indicates that at least some processing and assembly occur within 3 h. However, labeled pentamers were still observed at the conclusion of the 18-h chase, suggesting a protracted cleavage of polyproteins synthesized during the labeling period. In contrast, labeled virions accumulate steadily over a period of 12 to 18 h after removal of label (Fig. 6) and are only barely detectable without any chase (2). This delay compared with the coincident accumulation of RNA and infectious virus is consistent with the hypothesis of RNA synthesis being rate limiting for HAV replication.

Surprisingly, procapsids were found to accumulate at a rate similar to that of virions, whereas if RNA synthesis were the only rate-limiting factor, it would be expected that large amounts of procapsids would accumulate, as seen in PV-infected cells treated with guanidine (4, 25). However, the role of procapsids as an intermediate in capsid assembly has been challenged by Pfister et al. (19), who suggest that PV empty capsids are an artifact of solubilization methods, while Rombaut and Boyé (21) showed that PV pentamers aggregate to form virions without significant amounts of empty capsids being detected as an intermediate. The formation of procapsids may occur as a result of the self-assembly of pentamers once the concentration reaches the stable level observed, but these self-assembled procapsids may be labile and fail to accumulate to high levels. Consistent with this, Ruchti et al. (24) report that procapsids of HAV are sensitive to freezing and thawing unless stabilized in 22% sucrose, and other studies have also suggested that these particles are more labile than intact virions (31).

The observation of the 100-kDa putative 13S pentamers in larger amounts at 18 rather than 36 h p.i. (Fig. 2A) suggests an alternative mechanism for the restriction in pentamer (and also procapsid) accumulation. Primary cleavage at the P12A-2B junction is reported to be catalyzed by HAV 3C in *trans* in a cell-free system (9) but is more likely to be in *cis* in intact cells, rapidly producing the 100-kDa monomer regardless of the free 3C concentration. This 100-kDa monomer can then assemble into the 13S species observed, followed by cleavage in *trans* to yield 14S pentamers of PX,

VP0, and VP3. However, in the presence of high concentrations of 3C, the *trans* cleavage of P12A may be more rapid than assembly, and the monomeric PX, VP0, and VP3 thus formed may then be degraded rather than assembled.

The coincident accumulation of infectious virus, RNA, and antigen in HAV-infected cells (Fig. 1) led to the hypothesis that RNA synthesis was rate limiting for virus production (3). It was not known, however, whether protein synthesis and processing might also contribute to the restricted replication of HAV. The results presented here suggest that protein processing involved in the production of pentamers is protracted (Fig. 2B) but not rate limiting for the production of infectious virus. Figures 3 and 4 clearly show the period of highest radiolabel uptake (synthesis of proteins which are ultimately assembled into stable particles) occurring from 6 to 9 h (procapsids) and 12 to 15 h p.i. (virions). Profiles for parameters of viral growth were found to increase at the start of the period of peak label uptake into virions, with maxima coinciding at 27 h p.i. (Fig. 1). This observed lag of at least 12 h can be considered significant when similar experiments on PV yielded a lag of about 5 h (Fig. 5) (12) and presumably reflects the protracted processing of HAV polyprotein into 14S pentamers combined with limited RNA synthesis.

We present one possible model to account for the observed kinetics of HAV protein synthesis, processing, and assembly (Fig. 7). Early after infection (up to 12 h p.i.) very little RNA is available for encapsidation, 3C protease levels are low, and processing of the polyprotein in *cis* yields pentamers of 13S (P12A). Further processing to 14S (PX, VP0, and VP3) must occur in *trans* and is gradual over the next 9 to 12 h (Fig. 2B), perhaps because of low levels of 3C in the cell (29). Polyproteins synthesized from 6 to 9 h p.i. are thus processed before RNA levels have increased greatly (Fig. 1), and empty capsid formation is therefore most efficient. Polyproteins synthesized from 12 to 15 h, however, are processed into pentamers at a time when RNA levels are high and rapidly increasing, favoring the production of virions. Polyproteins synthesized after 18 h may be processed more rapidly in *trans*, but the pool of pentamers is now large and in excess of the RNA available for encapsidation; hence, new pentamers are less likely to be assembled into virions. With such an excess of pentamers, self-assembly into procapsids would be expected to increase but is in fact less efficient at these times (Fig. 3 and 4). This may reflect rapid processing of P12A monomers to PX, VP0, and VP3 by 3C in *trans* and subsequent degradation, rather than assembly into 13S pentamers (P12A) and subsequent processing in *trans* into 14S (PX, VP0, and VP3) pentamers and assembly into procapsids and virions. Further experiments are required to test this hypothesis; in particular, we intend to examine the relative levels of 13S and 14S pentamers early in infection and the stability of labeled procapsids and pentamers.

As this study has concentrated on viral structural proteins, it must be considered that the processing of nonstructural proteins may be limiting replication. Updike et al. (29) noted that in cells persistently infected with HAV, the levels of nonstructural proteins never accumulated to levels seen for capsid proteins. Determination of viral RNA-dependent RNA polymerase activity during a single growth cycle would be one way of testing for the delayed appearance of a nonstructural protein necessary for replication. Similarly, a delay in the production of mRNA (perhaps because of the inefficient removal of the genome-linked protein, VPg) could also be contributing to some of the unusual replication kinetics observed in this study. To this end, a method for the isolation of HAV mRNA (7) will be useful in studies planned to elucidate more detailed kinetics of synthesis and assembly for the HAV-specific macromolecules detected in this study.

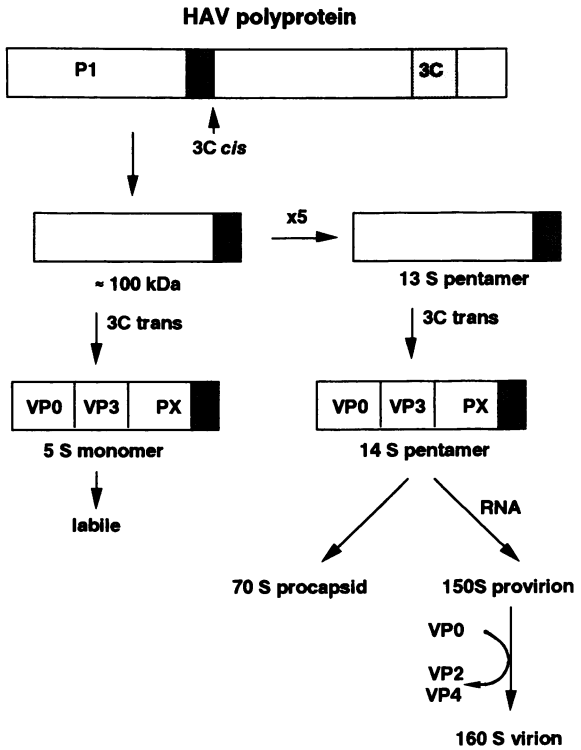


FIG. 7. Proposed model of the processing and assembly of HAV capsid proteins. The polyprotein is first cleaved in *cis* by 3C to yield P12A. Early in infection when 3C levels are low, these P12A monomers self-assemble to form 13S pentamers with subsequent cleavage by 3C in *trans* to yield 14S pentamers containing PX, VP0, and VP3. These particles can then self-assemble to form either empty capsids (in the absence of RNA) or virions (when RNA is present). Late in infection, higher levels of 3C lead to the cleavage of most P12A in *trans* before assembly into pentamers, and the monomeric PX, VP0, and VP3 subunits cannot then self-assemble into pentamers, virions, or procapsids and are degraded.

## ACKNOWLEDGMENTS

We thank John Mills and Ian Holmes for critical reading of the manuscript, Naomi Bishop and Sotirios Kolivas for helpful discussions, and Danielle Hugo and Patrick Edwards for excellent technical assistance.

S.V.B. is supported by a University of Melbourne postgraduate research scholarship. This work was supported in part by the World Health Organisation Programme for Vaccine Development and the B.H.P. Community Trust.

## REFERENCES

1. **Anderson, D. A.** 1987. Cytopathology, plaque assay, and heat inactivation of hepatitis A virus strain HM175. J. Med. Virol. **22**:35–44.
2. **Anderson, D. A., and B. C. Ross.** 1990. Morphogenesis of hepatitis A virus: isolation and characterization of subviral particles. J. Virol. **64**:5284–5289.
3. **Anderson, D. A., B. C. Ross, and S. A. Locarnini.** 1988. Restricted replication of hepatitis A virus in cell culture: encapsidation of viral RNA depletes the pool of RNA available for replication. J. Virol. **62**:4201–4206.

3a. **Borovec, S. V., and D. A. Anderson.** Unpublished data.

4. **Cho, M. W., and E. Ehrenfeld.** 1991. Rapid completion of the replication cycle of hepatitis A virus subsequent to reversal of guanidine inhibition. Virology **180**:770–780.
5. **Cohen, J. I., J. R. Ticehurst, S. M. Feinstone, B. Rosenblum, and R. H. Purcell.** 1987. Hepatitis A virus cDNA and its RNA transcripts are infectious in cell culture. J. Virol. **61**:3035–3039.
6. **Coulepis, A. G., G. A. Tannock, S. A. Locarnini, and I. D. Gust.** 1981. Evidence that the genome of hepatitis A virus consists of single-stranded RNA. J. Virol. **37**:473–477.
7. **de Chastonay, J., and G. Siegl.** 1987. Replicative events in hepatitis A virus-infected MRC-5 cells. Virology **157**:268–275.
8. **Gauss-Müller, V., and F. Deinhardt.** 1984. Effect of hepatitis A virus infection on cell metabolism *in vitro*. Proc. Soc. Exp. Biol. Med. **175**:10–15.
9. **Harmon, S. A., W. Updike, X.-Y. Jia, D. F. Summers, and E. Ehrenfeld.** 1992. Polyprotein processing in *cis* and in *trans* by hepatitis A virus 3C protease cloned and expressed in *Escherichia coli*. J. Virol. **66**:5242–5247.
10. **Jackson, R. J.** 1986. A detailed kinetic analysis of the *in vitro* synthesis and processing of encephalomyocarditis virus products. Virology **149**:114–127.
11. **Jia, X.-Y., E. Ehrenfeld, and D. F. Summers.** 1991. Proteolytic activity of hepatitis A virus 3C protein. J. Virol. **65**:2595–2600.
12. **Korant, B. D.** 1977. Protein cleavage in virus-infected cells. 1977. Acta Biol. Med. Ger. **36**:1565–1573.
13. **Laemmli, U. K.** 1977. Cleavage of structural proteins during the assembly of the head of bacteriophage T4. Nature (London) **227**:680–685.
14. **Lemon, S. M.** 1992. Hepatitis A virus: current concepts of the molecular virology, immunobiology and approaches to vaccine development. Rev. Med. Virol. **2**:73–87.
15. **Lemon, S. M., L. N. Binn, and R. H. Marchwicki.** 1983. Radioimmunofocus assay for quantitation of hepatitis A virus in cell cultures. J. Clin. Microbiol. **17**:834–839.
16. **Locarnini, S. A., A. G. Coulepis, E. G. Westaway, and I. D. Gust.** 1981. Restricted replication of human hepatitis A virus in cell culture: intracellular biochemical studies. J. Virol. **37**:216–225.
17. **McGregor, S., L. Hall, and R. R. Rueckert.** 1975. Evidence for the existence of protomers in the assembly of encephalomyocarditis virus. J. Virol. **15**:1107–1120.
18. **McGregor, S., and R. R. Rueckert.** 1977. Picornaviral capsid assembly: similarity of rhinovirus and enterovirus precursor subunits. J. Virol. **21**:548–553.
19. **Pfister, T., M. Troxler, D. Egger, and K. Bienz.** 1992. Immunocytochemical localisation of capsid related particles in subcellular fractions of poliovirus-infected cells. Virology **188**:676–684.
20. **Putnak, J. R., and B. A. Phillips.** 1981. Picornaviral structure and assembly. Microbiol. Rev. **45**:287–315.
21. **Rombaut, B., and A. Boyé.** 1990. New evidence for the precursor role of 14 S subunits in poliovirus morphogenesis. Virology **177**:411–414.
22. **Ross, B. C., B. N. Anderson, and I. D. Gust.** 1988. Expression of the hepatitis A virus genome as β-galactosidase fusion proteins in *Escherichia coli*, p. 62–64. *In* A. J. Zuckerman (ed.), Viral hepatitis and liver disease. Alan R. Liss Inc., New York.
23. **Ross, B. C., and D. A. Anderson.** 1991. Characterisation of hepatitis A virus capsid proteins with antisera raised to recombinant antigens. J. Virol. Methods **32**:213–220.
24. **Ruchti, F., G. Siegl, and M. Weitz.** 1991. Identification and characterisation of incomplete hepatitis A virus particles. J. Gen. Virol. **72**:2159–2166.
25. **Rueckert, R. R.** 1990. Picornaviruses and their replication, p. 507–548. *In* B. N. Fields, D. N. Knipe, R. M. Chanock, J. L. Melnick, B. Roizman, M. S. Hirsch, and J. P. Monath (ed.), Virology. Raven Press, New York.
26. **Saborio, J. L., S. S. Pong, and G. Koch.** 1974. Selective and reversible inhibition of protein synthesis in mammalian cells. J. Mol. Biol. **85**:195–211.
27. **Scholz, E., U. Heinricy, and B. Flehmig.** 1989. Acid stability of hepatitis A virus. J. Gen. Virol. **70**:2481–2485.
28. **Siegl, G., M. Weitz, and G. Kronauer.** 1984. Stability of hepatitis A virus. Intervirology **22**:218–226.
29. **Updike, W. S., M. Tesar, and E. Ehrenfeld.** 1991. Detection of hepatitis A virus proteins in infected BS-C-1 cells. Virology **185**:411–418.
30. **Vakharia, V. N., M. A. Devaney, D. M. Moore, J. J. Dunn, and M. J. Grubman.** 1987. Proteolytic processing of foot-and-mouth disease virus polyproteins expressed in a cell-free system from clone-derived transcripts. J. Virol. **61**:3199–3207.
31. **Winokur, P. L., J. H. McLinden, and J. T. Stapleton.** 1991. The hepatitis A virus polyprotein expressed by a recombinant vaccinia virus undergoes proteolytic processing and assembly into viruslike particles. J. Virol. **65**:5029–5036.